



Contents lists available at ScienceDirect

Sensors and Actuators B: Chemical

journal homepage: www.elsevier.com/locate/snb



Research paper

A power compensated differential scanning calorimeter for protein stability characterization

Shuyu Wang^a, Shifeng Yu^b, Michael Siedler^c, Peter M. Ihnat^d, Dana I. Filoti^d, Ming Lu^e, Lei Zuo^{b,*}

^a Department of Mechanical Engineering, Stony Brook University, Stony Brook, NY 11794, USA

^b Department of Mechanical Engineering, Virginia Tech, Blacksburg, VA, 24061, USA

^c AbbVie, Deutschland, 67061 Ludwigshafen, Germany

^d AbbVie Bioresearch Center, Worcester, MA 01605, USA

^e Center for Functional Nanomaterials, Brookhaven National Laboratory, Upton, NY 11973, USA

ARTICLE INFO

Article history:

Received 13 June 2017

Received in revised form

12 September 2017

Accepted 5 October 2017

Available online xxx

Keywords:

Microcalorimeter

Protein stability

Differential scanning calorimeter

ABSTRACT

This paper presented a power compensated MEMS differential scanning calorimeter (DSC) for protein stability characterization. In this microfabricated sensor, PDMS (Polydimethylsiloxane) and polyimide were used to construct the adiabatic chamber ($1\text{ }\mu\text{L}$) and temperature sensitive vanadium oxide was used as the thermistor material. A power compensation system was implemented to maintain the sample and reference at the same temperature. The resolution study and step response characterization indicated the high sensitivity (6 V/W) and low noise level ($60\text{ }\mu\text{k}$) of the device. The test with IgG1 antibody (mAb1) samples showed clear phase transitions and the data was confirmed to be reasonable by comparing it with the results of commercial DSC's test. This device used $\sim 1\text{ }\mu\text{L}$ sample amount and could complete the scanning process in 4 min, significantly increasing the throughput of the bimolecular thermodynamics study like drug formulation process.

© 2017 Elsevier B.V. All rights reserved.

1. Introduction

Protein stability is of great interests in the protein-based pharmaceutical formulation. When macromolecules, like the proteins, undergo temperature change, they transform from the native state to the denatured state. The higher this thermal transition midpoint (T_m) is, the more stable the molecules are. Differential scanning calorimeters (DSC) are often used to study this thermal transition phenomenon since they reveal the mechanism of thermostability by showing the temperature dependence of the protein transitions in the native forms [1]. It measures the heat change associated with the molecule's thermal denaturation when heated at a constant speed so that T_m and enthalpy change (ΔH) can be obtained simultaneously. These data from the calorimeter provide vital information for the formulation of therapeutic candidates.

However, accurate DSC measurements with a small amount of liquid protein sample are challenging due to the low enthalpy change during the phase transition. Researchers and engineers have been developing various approaches to improve the DSC's per-

formance for decades. Conventional commercial DSCs use pans, capillaries or tubes to construct the chambers. They serve to hold the liquid, prevent evaporation and provide a thermal isolated environment. One advantage of the bulk chamber is they can withstand additional pressure to suppress sample evaporation and prevent air bubbles at a higher temperature, so that the measurements are more repeatable. Recent exploration of AC DSC [2] and TMDSC (temperature modulated differential scanning calorimeter) [3] in the academia also pave a way to improve the DSC instruments. They use an averaging technique to extract the signal from the broad band noise, and some have reported the thermal unfolding of the lysozyme sample been detected [4,5]. Despite the techniques used, conventional DSCs still suffer from large sample volume (typically $300\text{ }\mu\text{L}$ – 2 mL) and long measurement time (typically 2 h).

Microfabrication can be an opportunity to improve the DSC. The suspended thin film either made of polymers [6–8] or Si_3N_4 [9–13] can be much more adiabatic and the smaller scale allowed far less sample amount. As a result, a higher sensitivity [14,15] was obtained. Meanwhile, due to the smaller temperature gradient in the sample region and the smaller addenda mass of the temperature sensor, it can detect the transition temperature more accurately. Moreover, embedded microheaters and ultra-small amounts of samples [16] made ultra-fast scanning possible. When the sample

* Corresponding author.

E-mail address: leizuo@vt.edu (L. Zuo).

is scanned at 1000 K/s, the power signal was magnified significantly since the power is proportional to the scanning rate. Meanwhile, a higher throughput can be achieved as a result of a shorter scanning time and parallel operation. This is crucial to the pharmaceutical industry, considering testing millions of drug candidates could take years to finish, even if automated systems are installed to perform the task consistently [17]. Last, microfabrication make low cost and massive production possible so that micro-DSCs might be disposable and wouldn't require a cleaning after the test.

However, the micro-DSC applied for protein stability characterization also confronts new challenges. The lower sample amount at the same concentration means a smaller power change during the denaturation, thus, it requires a more sensitive sensor. Meanwhile, the smaller thermal mass of biological sample can be more susceptible to evaporation at high temperatures even if plastic covers [6,18] are used. This loss of heat capacity can be detrimental to the measurement and limit the applications. And, if the chamber is totally sealed, the rising temperature can lead to higher pressure which is hard for the thin film to withstand. Apart from these, since DSC used differential measurement, the asymmetry between the sample and reference side can be crucial to the baseline performance. A slight difference can result in a large mismatch between the two sides, especially when the fabrication scale shrinks. Previous attempts on heat flux type DSC for this application were reported [7]. They determined the power by the sensitivity calibration using a known power and measuring the signal output. However, during the scanning the thermal conductance could slightly change since it could be temperature dependent [19]. This might result in an inaccurate measurement (see Eq. (3) therein). Currently, power compensated type of microfabricated DSC for the biological application remains scarce.

Here, we report a power compensated high performance micro-DSC. It was based on a polyimide flexible membrane and was bonded with an optimized PDMS microfluidic chamber (1 μL volume) for thermal insulation and evaporation suppression. It used vanadium oxide thermistors to monitor the slight temperature differences between the reference and sample side, which was maintained constant by the power compensation system. The power measured by the power compensation system was later converted to the normalized heat capacity changes [20]. We also constructed a temperature controlled heating stage to linearly raise the temperature and provide the thermal shielding for the microcalorimeter. To characterize the device, we analyzed the device resolution and used a power step response to calibrate the device. These demonstrated the microcalorimeter had a superb performance to test the protein samples. The IgG1 antibody (mAb1) showed a dynamic heat capacity change during the thermal denaturation. The T_m and ΔH was found reasonable by comparing it with the test data from a commercial DSC.

2. Device description

2.1. Microfabricated calorimeter sensors

Micro-DSC measurement required the biological sample and the reference solution in two identical chambers. The temperature was scanned simultaneously at a constant rate. Our sensor (Fig. 1) was mainly consisted of two parts: a PDMS microchamber and a sensor based on a polyimide substrate. The PDMS microfluidic chamber (1 μL volume) was fabricated by molding using an SU 8 master pattern (200 μm height). To improve the thermal insulation and reduce the addenda mass, the chamber was surrounded by air gaps. The flexible sensor fabrication started from spinning coating liquid polyimide (PI 2611, HD Microsystems) and heat treatment. After the microheater fabrication by lithography [21], a PI dielec-

tric layer was coated. The vanadium oxide thin film was sputtered evenly on the polymer, followed by metallization of the thermistors by photolithography. The metal traces were parallel connected with 10 μm gaps between them to obtain a moderate resistance (20–50 $\text{K}\Omega$). Within the sensing area and reference area, four thermistors were connected by metal wires as a Wheatstone bridge detect the minor temperature difference between the two sides. Note that the thermistors' resistance had to be very close to each other (<2% difference) so that the differential measurement could be performed, or else the signal readout would have a large offset and the scanning would also introduce a slope, making the small signal detection even harder. Then, we coated a layer of PI to protect the thermistor material from the water hydrolyzation. The PDMS microchamber was bonded firmly with the flexible sensor by the adhesive epoxy using the stamp-and-stick method [22].

2.2. Theories and power compensation control diagrams

The microcalorimeter's thermal model can be simplified as a one order system when only the sample area is considered. It is described by the differential equation:

$$C_p \frac{dT}{dt} + G \cdot (T - T_0) = P \quad (1)$$

where G is the thermal conductance of the chamber, C_p is the heat capacity, T is the temperature, and P is the power.

Since the four thermistors were connected as a Wheatstone bridge, the voltage difference (ΔV) of the two sides induced by temperature difference (ΔT) can be described by

$$\Delta V = \frac{1}{2} \alpha V_{in} \Delta T \quad (2)$$

where α is the temperature coefficient of resistance (-2.5%), V_{in} is the voltage input of the bridge (0.5 V). The temperature sensitivity is 5–7 mV/K.

At the steady state, ΔT and ΔP have the following relationship:

$$\Delta T = \frac{\Delta P}{G} \quad (3)$$

Combining Eqs. (2) and (3), the sensitivity (S) can also be calculated as

$$\Delta V = S \cdot \Delta P \quad (4)$$

By approximation, we can convert the power difference to heat capacity difference using the following equation:

$$\Delta C_p = \frac{\Delta P}{\beta} \quad (5)$$

Here β is the scanning rate.

Power compensated DSCs normally have two control loops: average temperature loop and differential temperature loop [23]. The average temperature loop delivers equal power to sample and reference sides to ensure that the average temperature tracks the program temperature. Meanwhile, the differential control loop minimizes the temperature difference between the sample and reference positions.

Fig. 2 shows how the power compensation system maintains a constant temperature difference between the sample and reference side. This study proposed a simplified control scheme. The error of the setpoint (V_{set}) and the output voltage (V_{out}) will firstly go through a PID controller and then it will multiply a constant k (the inverse of sensitivity), to determine how much power to compensate. This compensated power (P_{comp}) together with the differential power to the sample and reference areas which is caused by the uneven heating determine the output voltage. The controller will adjust power when outside disturbances are involved. In this way, the V_{out} will remain constant due to the feedback control.

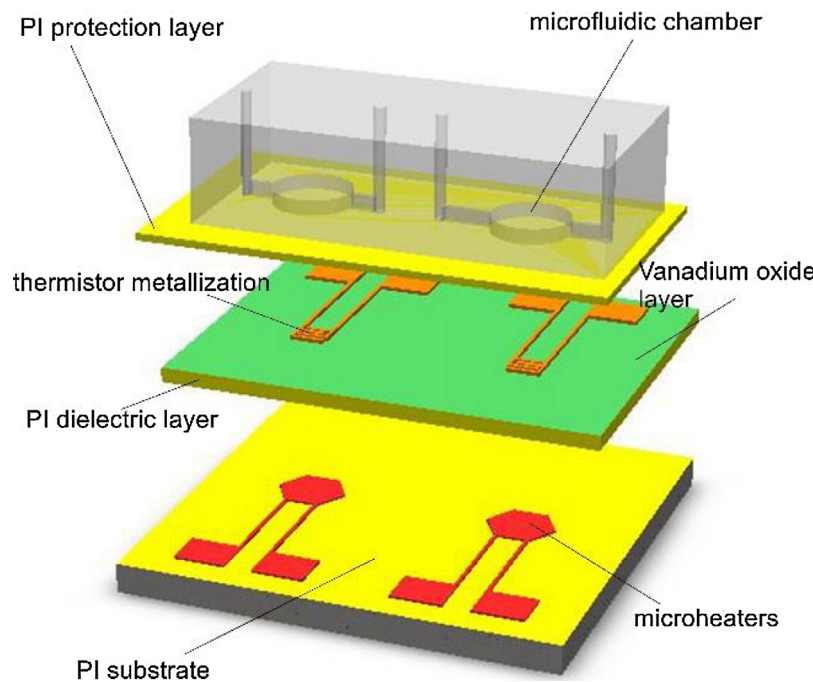


Fig. 1. A schematic view of the micro-DSC sensor. Each major layers were separated to illustrate the components.

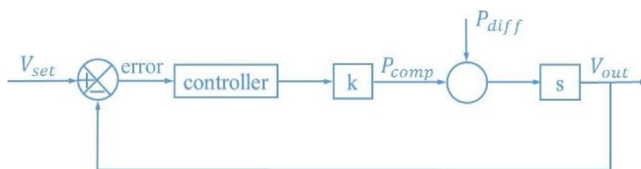


Fig. 2. The control diagram of the differential temperature control loop in the power compensation system. The feedback power from the microheater maintains a constant temperature between the sample and reference sides.

2.3. Heating stage of the calorimeter and electronic chains of the system

The heating stage of the microcalorimeter was constructed to raise the temperature and provide the thermal shielding. This corresponded to the average control temperature loop. The hardware included a heating sink, a copper plate, two Peltier heaters, a sample stage, a glass cover, the thermal shielding (made of Teflon tube), and the metal shielding. The two-layer shielding blocked the outside disturbance and minimized the temperature fluctuation. The wires were connected outside via a hole on the sample stage and then soldered to an electrical box with BNC adapters. The heaters were controlled by a temperature controller TC-720 (TE Tech) and powered by a power supplier. A commercial thermistor sensor was attached to the sample stage to measure the temperature. The temperature control process is automated by a commercial program (*Figs. 3 and 4*).

The power compensation system's electronic chain (*Fig. 5*) started from the lock-in amplifier (Stanford Research SR830) sending the voltage input to the Wheatstone bridge circuit and the differentiated signal (ΔV) was also measured by it. This signal was read by the LabVIEW program, and then the software controlled the sourcemeter (Keithley 2410) to release the power through the microheater to perform the power compensation. The amount of power to use was determined by the algorithm showed in *Fig. 2*. Since the resistance of the heater changed when temperature change, the sourcemeter need to measure the resistance in every cycle and set the sourcemeter's voltage according to the resistance

measured and the power value. The PID controller used in the study was from the NI company's control kit. All the data communication was achieved by the GPIB cable.

3. Experiments and materials

During the measurement, the microcalorimeter was suspended by an aluminum board drilled with holes. The silicone paste was used in between to improve the thermal contact between the board and the sensor. We slowly injected the liquid sample into the microchamber with a syringe and make sure no air was trapped in the chamber. If air was left in the chamber, it will swell when heated up, causing troubles in measurement. To reduce the chance of air introduction, the chamber was made hydrophilic by plasma treatment, the geometry was optimized to prevent the air trapped in the corner, and the liquid needed to be degassed. The inlet and outlet of the microchamber was sealed by the water-proof gel to further reduce evaporation. Five minutes after the injection, the temperature of the sample gradually came to equilibrium, and the temperature controller was turned on to scan the sensor at a rate of 25 K/min. The time constant of the lock-in amplifier was set to 300 ms, corresponding to a filter bandwidth of around 0.8 Hz. The V_{in} was set to be 0.5 V, so the power difference generated by the thermistors was much smaller than 1 μ W while maintaining a high sensitivity. We used a microfabricated heater powered by the sourcemeter to apply a little amount of heat to the sample for the thermal response study.

The protein test used the 10 mg/mL IgG1 antibody (mAb1) sample, prepared by the AbbVie company (Worcester, MA). The buffer used was filtered 15 mM Histidine pH 6. In each measurement, the baseline drift was subtracted from the data to yield the net signal.

The commercial thermal analysis instrument used for comparisons was the VP-capillary DSC from Malvern Instruments.

4. Results and discussions

Thermal response tests were often used to calibrate the calorimeter and to show how the sensor react to a small amount

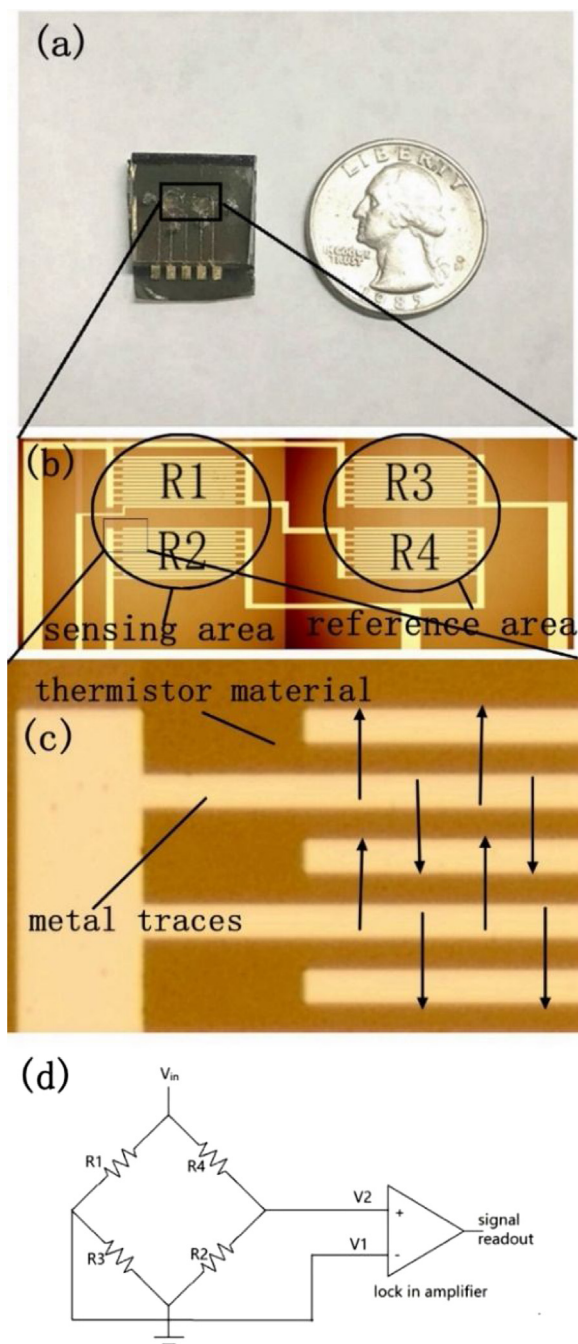


Fig. 3. (a) Photograph of the microcalorimeter sensor (b) image of the reference and sensing areas optical microscope (c) image of the metal traces under optical microscope to illustrate how it connected the thermistor materials to reach a reasonable resistance. The arrow in the picture was the current flow direction (d) schematic diagram of the electrical connection s between the four thermistors to perform differential measurement.

of heat. It was operated by applying a known power for a certain time and read the voltage signal. By integrating the voltage signal with time and dividing it by the heat applied, the sensitivity could be determined. It also characterized the sensor's performance on thermal insulation and time constant based on Eq. (1).

Fig. 6 showed the situation when 400 μW power was applied and 1 μL of DI water was loaded in the microchambers. Integrating the voltage over time and dividing the known heat revealed a 6 V/W sensitivity. By fitting the rising curve and downward curve to the exponential equation, we found the time constant to be 7.2 s, which

Table 1

Comparison of the proposed MEMS DSC and the commercial DSC in protein sample study.

Commercial DSC/MEMS DSC	mAb1	Lysozyme	BSA
T_m ($^{\circ}\text{C}$)	74.3/75.4	78.8/79.3	77.5/76.7
ΔH (kJ/mol)	431/385	920/862	2234/2444

Table 2

Lists of most up-to-date MEMS DSC works for liquid sample study.

MEMS DSC work	Sample consumption	Sensitivity	Noise level
Zuo's group	1 μL	6 V/W	35 nW/60 μK
Lin's group, [8]	1 μL	4.78 V/W	20 nW
Saito and Nakabepu, [25]	Flow through		100 nW

was quite similar to some commercial products (time constant of VP-DSC is 7 s).

To enlighten the performance of the calorimeter, the noise study of the device was also conducted. Signal readout in the lock-in amplifier was recorded when the microcalorimeter was scanned at 25 K/min. We subtracted the raw data with a three order polynomial fit, and then convert the residual to the power and the heat capacity (Fig. 7). The peak to peak noise of the calorimeter was around 250 nJ/K (based on the equation 5), corresponding to 100 nW; the RMS (root mean square) noise was about 85 nJ/K and 35 nW. Considering the heat capacity of the sample 4.2 mJ/K, the resolution was approximately $\Delta C/C = \pm 3 \times 10^{-5}$. Possible influencing factors could arise from the linearity of the temperature scanning control, the thermal shielding performance of the heating stage, and the thermal insulation of the device.

Besides, we also evaluated the power compensation performance of the feedback system. The signal output (ΔV) from the lock-in amplifier was set to maintain a constant by the high performance feedback control system. It meant the temperature difference of the two sides could remain the same during the. In Fig. 8, two consecutive tests were carried out and they showed high repeatability.

We studied the antibody mAb1 sample with 10 mg/mL concentration (molecular weight: 148000), which corresponds to 1% wt. The relationship between the heat capacity change and temperature was showed in Fig. 9. We subtracted the baseline and normalized the result based on the molecular weight. The transition temperature (T_m) detected by our device was around 75.4 $^{\circ}\text{C}$. The enthalpy change (ΔH) was calculated to be 2234 kJ/mol after integrating the normalized heat capacity. We then measured the sample with a commercial DSC and found T_m was 74.3 $^{\circ}\text{C}$ and ΔH was 2444 kJ/mol. Besides, we found the peak was narrower and the T_m was lower. We also used the microfabricated DSC to measure the denaturation process of lysozyme and BSA samples and compared the results with the commercial VP-DSC. The information such as volume, concentration and buffer selection were kept the same as the mAb1 study. The comparison results are showed in Table 1.

Potential explanations for these discrepancies may include that the micro-DSC had a much smaller volume (micro-DSCs used 1 μL sample and the commercial DSC's volume was 400 μL), rendering a faster heat dissipation process and a higher thermal uniformity. This meant that the thermal event might last shorter in the microchamber. Differences in T_m could also be related to the different scanning speed. The micro-DSC was scanned at 25 $^{\circ}\text{C}/\text{min}$ and the commercial DSC's scanning rate was 2 $^{\circ}\text{C}/\text{min}$. Such different scanning rates could also result in differences in the kinetics of protein denaturation[24]. Other factors like differences in biological sample preparation, the variability in sample concentrations and trace impurities in the protein sample might lead to differences in the detection as well. Despite these differences we found in the measurement, the micro-DSC was demonstrated to be able

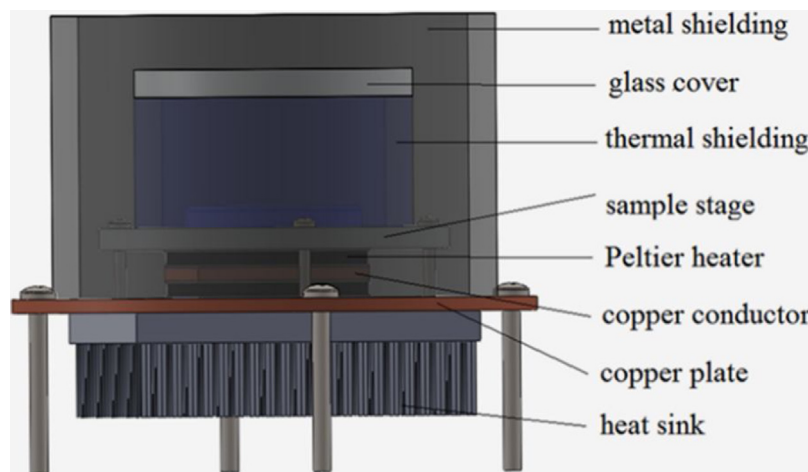


Fig. 4. Heating stage of the calorimeter. It was used to scan the calorimeter sensor and provide thermal shielding.

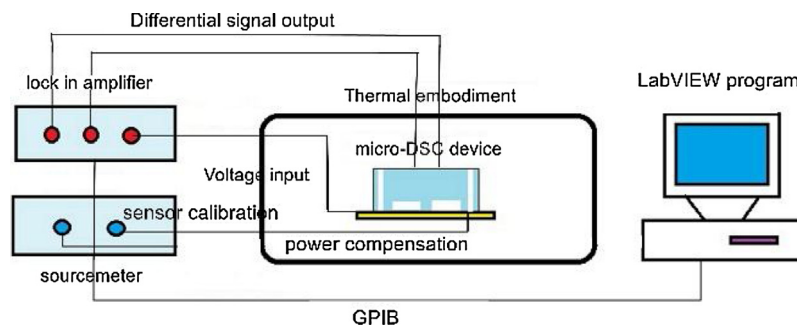


Fig. 5. electronic chain of the power compensation system.

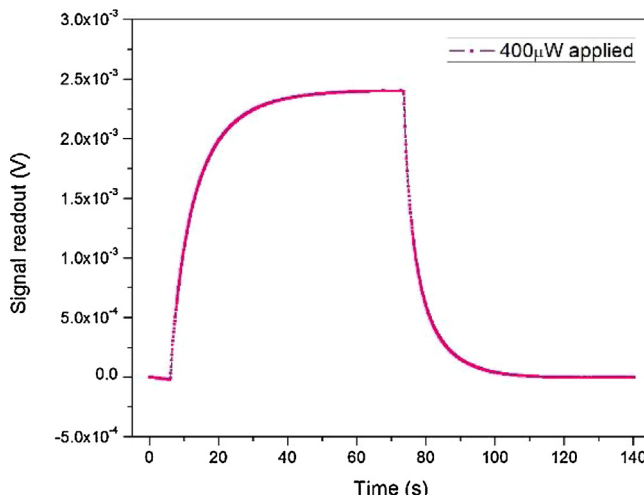


Fig. 6. (a) The step response study applying $400 \mu\text{W}$ with $1 \mu\text{L}$ water in the chamber. The sensitivity was determined to be 6 V/W .

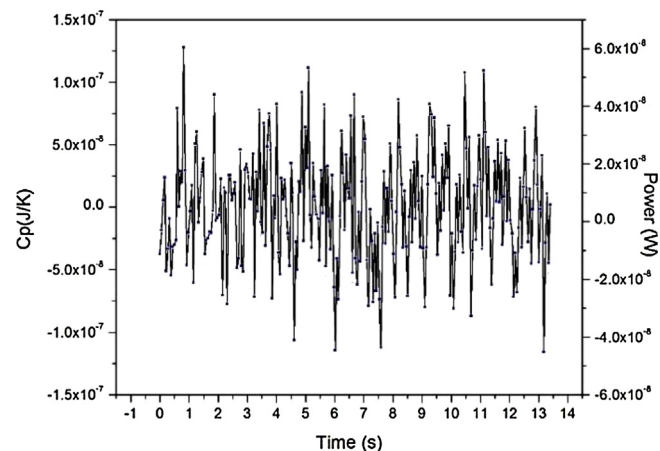


Fig. 7. resolution of the calorimeter regarding heat capacity and power.

to conduct thermal stability analysis of liquid protein samples. It consumed much less protein sample and could greatly improve the throughput by enabling faster scans and parallel operations. This instrument may be incorporated into high throughput screening workflows for the relative comparison of thermal properties between large numbers of proteins when only small quantities are available.

The progress in the development of chip based differential scanning calorimeters for liquid sample study is showed in Table 2. Although there have been a lot of reports about developing micro

DSCs, only a few targeted on liquid sample characterization due to the vital evaporation problem during the temperature scanning process. Compare to the two other DSCs which utilized thermopile for temperature sensing, the proposed MEMS based DSC is the first thermistor based micro calorimeter which could reach to a noise level of nanowatts. It shows our newly designed DSC is leading the way in protein study with ultra-low sample volume consumption, high sensitivity and ready for protein sample tests.

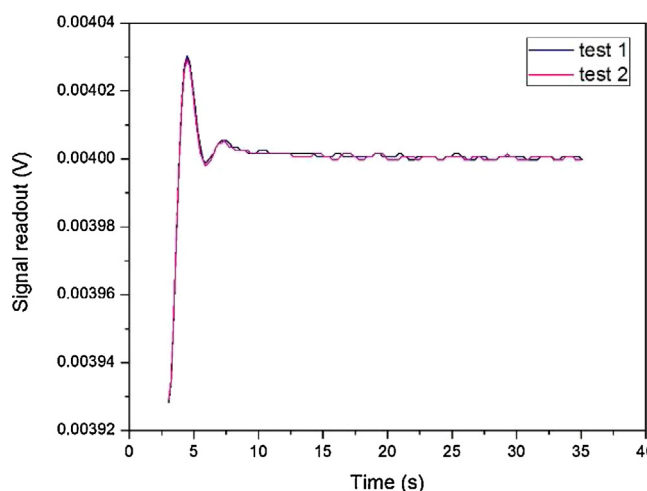


Fig. 8. power compensated baseline study. The power compensation system kept the signal readout ΔV to be a constant after the control, meaning the temperature difference ΔT is a constant during the process. Two consecutive tests of the baseline were compared for repeatability study.

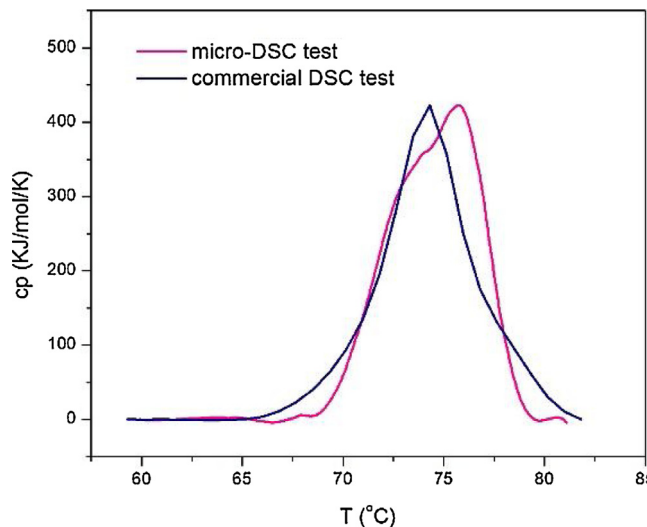


Fig. 9. comparison between commercial DSC and micro-DSC's test with the IgG1 antibody(mAb1). After baseline subtraction, the data was converted and normalized to heat capacity.

5. Conclusions and perspectives

Microfabricated DSCs for liquid protein stability studies confronts many challenges. This paper presented a high performance power compensation micro-DSC that addressed the technical difficulties. The optimized PDMS chamber ($1 \mu\text{L}$) and polyimide film led to low heat conduction and low evaporation. Ultrasensitive vanadium oxide thermistors monitored a slight temperature difference between the reference and sample region. A well-designed heating stage was built for linear scanning and shielding. A power compensation system achieved by LabVIEW program was made to maintain a constant temperature difference during scanning process. We studied the noise behavior of the device, which had a $250 \text{nJ}/\text{K}$ resolution. The step response study revealed a high sensitivity (6V/W) of the device and the ability for low power detection (the detectable power limit should be much smaller than the applied power ($400 \mu\text{W}$)). Furthermore, we moved on to the biological sample tests and detected the heat capacity change of the protein denaturation using an IgG1 antibody (mAb1) sample and other two protein samples. The result had been verified by a com-

mercial DSC. The performance of the micro DSC was also compared with other similar works in developing MEMS based DSC. Overall, the micro-DSC had the potential to characterize the thermal stability of protein with significantly higher throughput and lower sample consumption, which might lead to a reduction in the cost and time for the drug R&D in the pharmaceutical industry.

Acknowledgements

The authors thank the funding support from NSF (IDBR #1152415) and AbbVie Inc. The fabrication was carried out at the Center for Functional Nanomaterials (CFN) at Brookhaven National Laboratory, which is supported by the U.S. Department of Energy, Office of Basic Energy Sciences, under Contract No. DE-AC02-98CH10886.

References

- [1] C.M. Johnson, Differential scanning calorimetry as a tool for protein folding and stability, *Arch. Biochem. Biophys.* 531 (2013) 100–109.
- [2] J.L. Garden, E. Château, J. Chaussy, Highly sensitive ac nanocalorimeter for microliter-scale liquids or biological samples, *Appl. Phys. Lett.* 84 (2004) 3597.
- [3] C.C.G. Salvetti, C. Ferrari, E. Tombari, A modulated adiabatic scanning calorimeter (MASC), *Thermochim. Acta* 364 (2000) 11–22.
- [4] E.T.G. Salvetti, L. Mikheeva, G.P. Johari, The endothermic effects during denaturation of lysozyme by temperature modulated calorimetry and an intermediate reaction equilibrium, *J. Phys. Chem. B* 106 (2002) 6081–6087.
- [5] H. Yao, K. Ema, H. Fukada, K. Takahashi, I. Hatta, ac nanocalorimeter for measuring heat capacity of biological macromolecules in solution, *Rev. Sci. Instrum.* 74 (2003) 4164.
- [6] S. Wang, S. Yu, M.S. Siedler, P.M. Ihnat, D.I. Filotti, M. Lu, et al., Micro-differential scanning calorimeter for liquid biological samples, *Rev. Sci. Instrum.* 87 (2016) 105005.
- [7] L. Wang, B. Wang, Q. Lin, Demonstration of MEMS-based differential scanning calorimetry for determining thermodynamic properties of biomolecules, *Sens. Actuators, B* 134 (2008) 953–958.
- [8] Y. Jia, B. Wang, Z. Zhang, Q. Lin, A polymer-based MEMS differential scanning calorimeter, *Sensor Actuat. A: Phys.* 231 (2015) 1–7.
- [9] V. Mathot, M. Pyda, T. Pijpers, G. Vanden Poel, E. van de Kerkhof, S. van Herwaarden, et al., The Flash DSC 1, a power compensation twin-type, chip-based fast scanning calorimeter (FSC): First findings on polymers, *Thermochim. Acta* 522 (2011) 36–45.
- [10] S.L. Lai, G. Ramanathan, L.H. Allen, P. Infante, Z. Ma, High-speed (104 (C/s) scanning microcalorimetry with monolayer sensitivity (J/m²), *Appl. Phys. Lett.* 67 (1995) 1229–1231.
- [11] D.W. Denlinger, E.N. Abara, Kimberly Allen, P.W. Rooney, M.T. Messer, S.K. Watson, F. Hellman, Thin film microcalorimeter for heat capacity measurements from 1.5 to 800 K, *Rev. Sci. Instrum.* 65 (1994) 946–957.
- [12] B. Davaji, H. Jeong Bak, W.J. Chang, C. Hoon Lee, A novel on-chip three-dimensional micromachined calorimeter with fully enclosed and suspended thin-film chamber for thermal characterization of liquid samples, *Biomicrofluidics* 8 (May) (2014) 034101.
- [13] J. Koh, W. Lee, J.H. Shin, High-sensitivity chip calorimeter platform for sub-nano watt thermal measurement, *Sensor Actuat. A: Phys.* 241 (2016) 60–65.
- [14] B. Wang, Q. Lin, Temperature-modulated differential scanning calorimetry in a MEMS device, *Sens. Actuators B* 180 (2013) 60–65.
- [15] E. Iervolino, A.W. van Herwaarden, P.M. Sarro, Calorimeter chip calibration for thermal characterization of liquid samples, *Thermochim. Acta* 492 (2009) 95–100.
- [16] R. Splinter, A.W. van Herwaarden, I.A. van Wetten, A. Pfreundt, W.E. Svendsen, Fast differential scanning calorimetry of liquid samples with chips, *Thermochim. Acta* 603 (2015) 162–171.
- [17] W. Lee, Koh Lee, Development and applications of chip calorimeters as novel biosensors, *Nanobiosensors Dis. Diagnosis* (2012) 17.
- [18] B. Wang, Q. Lin, A MEMS differential-scanning-calorimetric sensor for thermodynamic characterization of biomolecules, *J. Microelectromech. Syst.* 21 (2012) 1165.
- [19] A.F. Lopeandía, L.L. Cerdó, M.T. Clavaguera-Mora, L.R. Arana, K.F. Jensen, F.J. Muñoz, et al., Sensitive power compensated scanning calorimeter for analysis of phase transformations in small samples, *Rev. Sci. Instrum.* 76 (2005) 065104.
- [20] Höhne Günther, F. Wolfgang Hemminger, H.-J. Flammersheim, *Differential Scanning Calorimetry*, Springer Science & Business Media, 2013.
- [21] Shifeng Yu, Shuyu Wang, Ming Lu, Lei Zuo, A novel polyimide based micro heater with high temperature uniformity, *Sensor Actuat. A: Phys.* (2017).
- [22] S. Satyanarayana, R.N. Karnik, A. Majumdar, Stamp-and-stick room-temperature bonding technique for microdevices, *J. Microelectromech. Syst.* 14 (2005) 392–399.

- [23] E. Zhuravlev, C. Schick, Fast scanning power compensated differential scanning nano-calorimeter: 1. The device, *Thermochim. Acta* 505 (2010) 1–13.
- [24] J.M. Sanchez-Ruiz, J.L. Lopez-Lacomba, M. Cortijo, P.L. Mateo, Differential scanning calorimetry of the irreversible thermal denaturation of thermolysin, *Biochemistry* 27 (1988) 1648–16522.
- [25] Masataka Saito, Nakabeppe Osamu, Flow type bio-chemical calorimeter with micro differential thermopile sensor, *J. Nanosci. Nanotechnol.* 15 (4) (2015) 2917–2922.

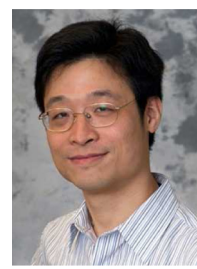
Biographies



Shuyu Wang is currently a PhD candidate in Stony Brook University. He got his bachelor degree in the Huazhong University of Science and Technology in the department of mechanical engineering. He is currently a third year PhD student in the mechanical engineering in Stony Brook University. His research interests include nanomaterials, MEMS sensors and calorimetry.



Dana I. Filoti is currently Senior Scientist II at AbbVie. She got her PhD in material science in University of New Hampshire in 2010.



Ming Lu is a staff scientist in the center of functional nanomaterials in Brookhaven National Lab. He got the bachelor degree in Fudan University, China and PhD in the department of physics and astronomy in Stony Brook University. His research focuses on the exploration of new methods and new materials for nanofabrication, especially for photonics and x-ray microscopy applications.



Shifeng Yu is currently a PhD candidate in Virginia Tech. He got his bachelor degree in the University of Science and Technology of China in the department of mechanical engineering. He then went to Stony Brook University to pursue a PhD degree in mechanical engineering and later transferred to Virginia Tech. His research interests include nanofabrication, MEMS based sensor and actuator, bio calorimetry.



Lei Zuo is an associate professor in the department of mechanic engineering in Virginia Tech. He got the bachelor degree from Tsinghua University and got the master degree together with the PhD in MIT. His research interests include thermoelectric materials and applications, bio sensors and instrumentation, large-scale energy harvesting from ocean waves, vehicle suspensions, civil structure vibration, railroad transportation, etc.



Michael Siedler is currently Head of NBE Formulation Development – bei AbbVie Deutschland GmbH & Co KG. He got his PhD in Chemistry in University of Hamburg in 2002.



Peter M. Ihnat is currently Principal Research Scientist/Group Leader at AbbVie. He got his PhD in Pharmaceutics in University of Nebraska Medical Center.